中國機械工程學刊第四十卷第三期第 257~262 頁(民國一百零八年)
Journal of the Chinese Society of Mechanical Engineers, Vol.40, No.3, pp 257~262 (2019)

Effects on Protein Preconcentration Using Nano-interstices via Self-assembled Monolayers with Different Concentrations of Au Nanoparticles

Ngoc-Viet Nguyen*, Meng-Syuan Wu*, Neng-Chuan Tien** and Chun-Ping Jen*

Key words: protein preconcentration, nanofracture, self-assembled monolayer, gold nanoparticles.

ABSTRACT

This study aimed to enhance the performance of a self-assembled monolayer of gold nanoparticles for a protein-preconcentration microchip that uses nanofractures generated by junction gap breakdown. Simple and low-cost techniques are applied to fabricate the chip. A mold master for the cross-shaped microchannels is created by the basic photolithography process on a silicon wafer. A suitable biocompatibility polydimethylsiloxane (PDMS) material is prepared and poured onto the mold master to replicate the channels. Subsequently, the glass substrate is silanized prior to functionalizing the gold nanoparticles at the designed region for self-assembly. The electrical breakdown voltage required for nanofracture generation is greatly reduced. The PDMS channel replica is bonded to the glass substrate using oxygen–plasma treatment. In the experiment, the chip is used to collect 10 μM Bovine serum albumin (BSA) labeled with fluorescein isothiocyanate (FITCBSA). Different concentrations of the gold-nanoparticle solution ranging from 1.325 nM to 26.5 nM are investigated. The optimal concentration of gold-nanoparticle solution is determined to be 1.325 nM. Furthermore, the concentration of FITC-labeled BSA at the desired region increases approximately 50 times from 10 μM to 0.5 mM in 15 min. These results demonstrate that a reliable method may be used to increase the concentration efficiency of the proposed chip.

Paper Received February, 2018. Revised March, 2018, Accepted April, 2018, Author for Correspondence: Chun-Ping Jen

* *Department of Mechanical Engineering, National Chung Cheng University, Chia-Yi 62102, Taiwan*

** *Nuclear Science and Technology Development Center, National Tsing Hua University, Hsinchu 30013, Taiwan*

INTRODUCTION

In recent years, the development of the microfluidic platforms has rapidly increased in biochemical device systems. Biological particle preconcentration has an important role that increases the sensitivity and accuracy of subsequent detection, especially for samples with extremely low concentrations (Lin, 2011). Among several potential approaches, the nanoporous membrane/nanochannel techniques have been used to preconcentrate proteins at low concentrations (Islam, 2013; Koh, 2017; Wang, 2015). Many methods have been strongly developed for the fabrication of nanochannels (Duan, 2013). Some devices with nanofluidic channels for protein manipulation have been fabricated using the standard photolithography and etching techniques (Wang, 2005; Wang, 2014; Wu, 2009). The polydimethylsiloxane (PDMS) techniques also offer the advantage of being able to integrate with protein-preconcentration microchips (Kim, 2006; Lee, 2008). A method using the junction-gap electrical breakdown between two PDMS microchannels has also been developed for the fabrication of nanofractures (Jeong, 2007), wherein a high direct-current (DC) voltage up to 1000 V was applied between microchannels 40 μm in width to create nanogaps. As a result, a concentration factor of 104 was obtained within 1 h. Using the same technique, Yu et al. (Yu, 2008) achieved a concentration factor of between 103 to 105 with the structure of two printed V-shaped microchannels, whereas Kim et al. (Kim, 2006) achieved a concentration factor of between 103 to 106 in 30 min for proteins.

A simpler electrokinetic protein sample preconcentrator has been reported in our studies (Chen, 2016; Jen, 2014) utilizing the similar

exclusion-enrichment effect in nanochannels (Pu, 2004). The creation of nanofractures at the junction gaps by deposition of gold nanoparticles allows a reduction in the required electrical breakdown voltage. As result of nonlinear electrokinetic flow, this effect causes the rapid accumulation of proteins in front of the induced ionic depletion zone. Overlapped electrical double layers in the microchannels enable the generation of ion-concentration polarization (Yang, 2015) under an electric field. This leads to ionic depletion on the anodic side of the channel. Thus, ions are enriched at one end and depleted at the other end of the channel. In previous research, the characteristics of nanogaps via the measurement of electrical properties have been investigated. The measurement of DC current as a function of applied voltage (I–V curve) has also been used to analyze the formation and dimensions of nanogaps. The experimental results revealed that a high concentration factor of 1.5×10^4 for fluorescein isothiocyanate (FITC)-labeled bovine serum albumin (BSA) with a low concentration of 1 nM was achieved in 30 min by using the proposed chip (Jen, 2015). In addition, an immunoassay of BSA and anti-BSA was also performed to demonstrate the applicability of the chip. An impedance measurement circuit board has been built integrated with the microchip for protein detection (Quoc, 2017). Sensing electrodes are located at the trapping region to confirm the presence of proteins. The method for nanofracture formation involves the effect of self-assembled monolayers (SAMs) of gold nanoparticles. Thus, the present study considers the changes in concentration of used gold nanoparticles. Based on experimental results, advanced conditions are suggested for the chip.

MATERIALS AND METHODS

Chip design and fabrication

The design and illustration of the microfluidic chip are shown in Fig. 1. The chip consists of a glass substrate and PDMS microchannels. The cross-shaped channel configuration has rectangular section dimensions with 100 µm width and 2 µm height. The horizontal channel concentrates protein toward the right side with a higher applied voltage. The vertical channel includes two junction gaps of 50 µm, which are symmetrical across the horizontal channel for the formation of nanofractures via electric breakdown. The self-assembly region of gold nanoparticles is the region between two above and below junction gaps, with length and width of 800 µm and 100 µm, respectively. This design allows the self-assembly zone of gold nanoparticles to cover the junction gaps of the vertical channel, and to reduce the error of bonding the PDMS channel. The microchip was fabricated using the standard photolithography process. First, the silicon wafer was cleaned with piranha solution (H_2SO_4: H_2O_2 with a volume ratio of 3:1) to remove surface organics, minerals, and other impurities. The cleaned wafer was then spin coated by S1813 photoresist (approximately 2 µm thick). After exposure and development, the mold master for defining the channel was created. A 10:1 weight mixture of PDMS prepolymer and curing agent (Sylgard-184 Silicone Elastomer Kit, Dow Corning, Midland, MI, USA) was poured and cured on the mold master to replicate the microchannel.

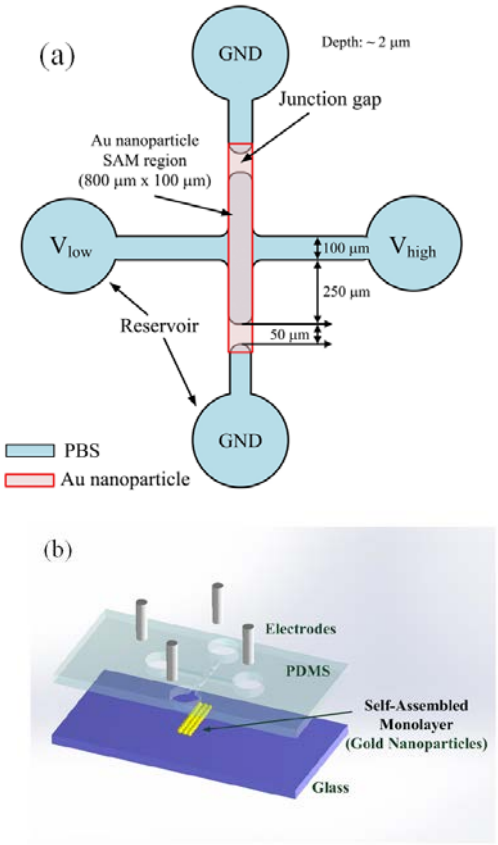

Fig. 1. Illustration of the protein sample preconcentration microchip: (a) Wafer design and its dimensions (b) 3D chip modeling.

After the PDMS replica had been peeled away, the inlet and outlet ports as well as the reservoirs were created using a puncher. A DC voltage was applied to the two anodic side reservoirs while the other reservoirs were grounded, thus initiating electric breakdown and form nanofractures (Fig. 1(b)). Fig. 2(a) shows the process of the surface modification. The rectangle region for the self-assembly of gold nanoparticles on the glass substrate was patterned using standard photolithography with S1813 photoresist. Silanization on the glass was achieved using 6 µL of 0.1% v/v (3-aminopropyl)triethoxysilane/DI water (APTES/H_2O) solution for 1 min. The glass substrate was then nitrogen dried after being rinsed in

deionized (DI) water, and reacted for 1 h in 20 µL of solution containing various gold-nanoparticle concentrations (1.325, 2.65, and 26.5 nM) for self-assembly. Subsequently, the glass underwent multiple rinses in acetone, methanol, and DI water to eliminate photoresist.

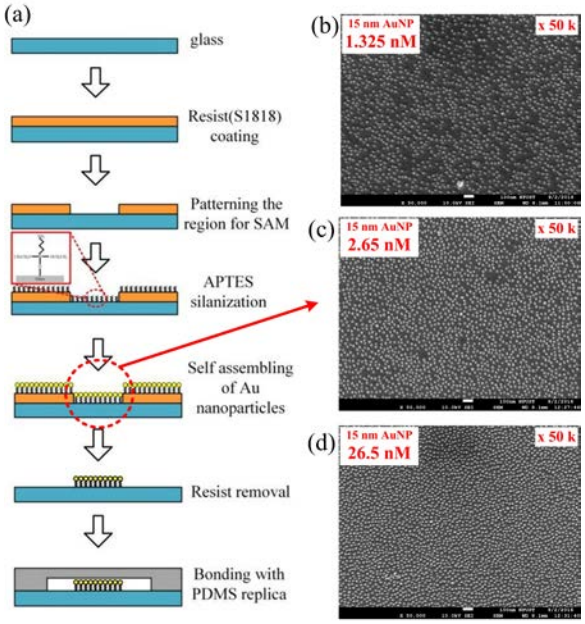

Fig. 2. (a) Schematic of self-assembly process of gold nanoparticle, and (b-d) SEM images of self-assembled monolayer with different gold-nanoparticle concentrations: (b) 1.325 nM, (c) 2.65 nM, and (d) 26.5 nM.

The mean diameter of gold nanoparticles used in this study was 15 nm. Figs. 2(b–d) show the self-assembled monolayers of gold nanoparticles with different concentrations captured using a scanning electron microscopy (SEM) system. After the nanoparticles had self-assembled in the designed region, the PDMS replica was bonded to the glass substrate using oxygen–plasma treatment in an O_2 plasma cleaner (PDC-32G, Harrick Plasma Corp., Ithaca, NY, USA). Four electrodes were then inserted into the reservoirs to apply the voltage required in the experiments.

Apparatus

Phosphate-buffered saline (PBS; 5 mM, pH 7.4) solution was used for the buffer system in this study. FITC-labeled BSA (Sigma–Aldrich, St. Louis, MO, USA), diluted in PBS at 10 µM concentration, was allowed to fill the microchannels via capillary force to demonstrate the on-chip protein preconcentration. A high-voltage power supply (Series 225, Bertan High Voltage Corp., Hicksville, NY, USA) provided the required voltages for junction gap breakdown and protein preconcentration. Protein preconcentration was then observed and recorded using an inverted fluorescence microscope (CKX41, Olympus, Tokyo, Japan) with a mounted CCD camera (DP71, Olympus, Tokyo, Japan) and connected to a computer running Olympus DP Controller image software. The excitation light source wavelength was 490 nm. The fluorescence intensities emitted by enriched FITC-labeled BSA were quantified using ImageJ software (National Institutes of Health, Bethesda, Maryland, USA), which can assess the density of each pixel.

Exclusion-enrichment effect (EEE), ion depletion effect, and electroosmotic flow (EOF) (Pu, 2004; Jen, 2015) are the main principles for protein preconcentration. Fig. 3 describes the protein-preconcentration process. FITC-labeled BSA and PBS buffer solution are initially injected into the microchannels. Nanofractures are created between the microchannels via junction gap breakdown when applying a high DC voltage. The same voltage of 50 V is applied to the two reservoirs (left and right ones), while the other reservoirs are kept at ground. Nanofractures at the junction gaps generate ion-enrichment and ion-depletion effects in the microchannels filled with PBS solution. This phenomenon induces nonlinear electrokinetic flow resulting in the EEE. A depletion region, which has no ions, is formed and extended gradually between two nanofractures until the self-assembly region is completely covered, as shown in Figs. 3(a–d).

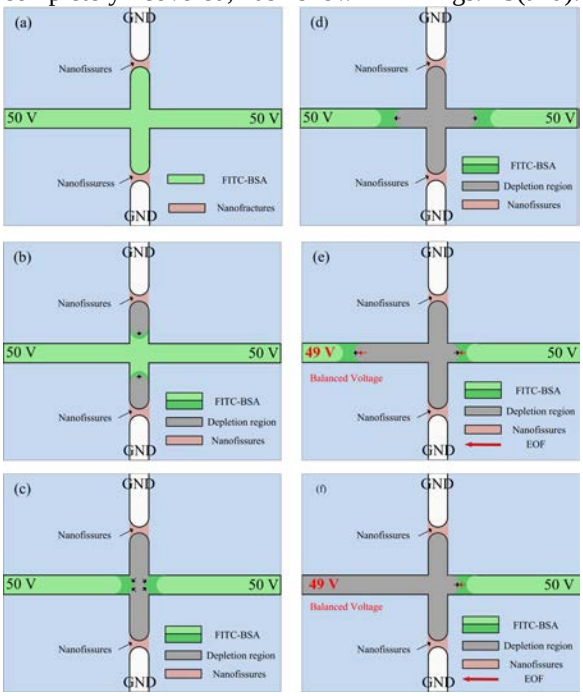

Fig. 3. Process of protein preconcentration based on the exclusion-enrichment effect, depletion effect, and electroosmotic flow principles.

Negatively charged ions (including protein particles) are pulled out of the depletion region and are collected into the horizontal channel. A lower voltage (49 V) is then applied to the left reservoir while maintaining the voltage of the right reservoir. The electroosmotic flow and ion-depletion effects are

thus formed continuously for moving protein particles toward the right side with the higher potential (Figs. 3(e and f)). As a result, the protein concentration is increased in the designed location at the microchannel by balancing the depletion force with the driving force produced by EOF.

RESULTS AND DISCUSSION

Gold nanoparticles with a mean size of 15 nm were used. The solutions with 1.325, 2.65, and 26.5 nM gold nanoparticles were adopted for self-assembly on the glass substrate. SEM images of the SAM at 1.325, 2.65, and 26.5 nM gold nanoparticles are shown in Figs. 2(b–d). The electric double layer thickness was achieved at 6.6752 nm, and the total size of the bilayer on the upper and lower walls was at 13.35 nm. Loose bonding around the self-assembled nanoparticles occurred due to the high density of nanoparticles underneath the junction gaps, which acted as a steric hindrance during PDMS bonding. However, a tight bonding formed with 1.325 nM gold nanoparticles, because the lower nanoparticle density created more space for the complete bonding between PDMS and the glass substrate (Fig. 4).

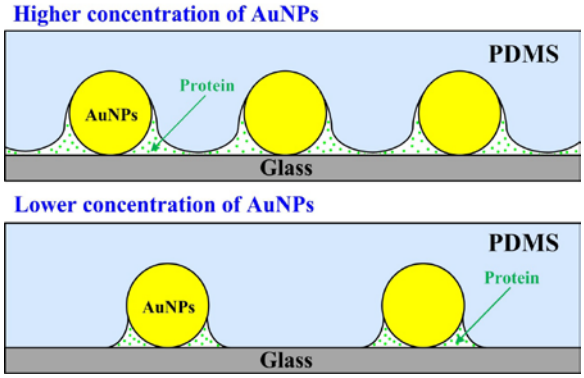

Fig. 4. Schematic of loose and tight bonding between PDMS replica and glass substrate with SAM of nanoparticles.

After forming the nanofractures, FITC-labeled BSA diluted in 5 mM PBS at 10 μM concentration was investigated and used to fill the microchannel via capillary force to perform the on-chip preconcentration of proteins. The operations of the electrokinetic protein preconcentration are presented in the above sections. Fluorescence images of 10 μM FITC-labeled BSA in 5 mM PBS solution taken at various time points (0, 5, 10, and 20 min) are shown in Fig. 5. Results indicate that BSA concentration and preconcentration-region size increased with time, which demonstrate that proteins can be concentrated using the proposed chip with SAMs of gold nanoparticles on a glass substrate underneath the junction gaps. The concentration of collected BSA proteins obtained from fluorescence intensity was quantified and averaged over a rectangular window using ImageJ software.

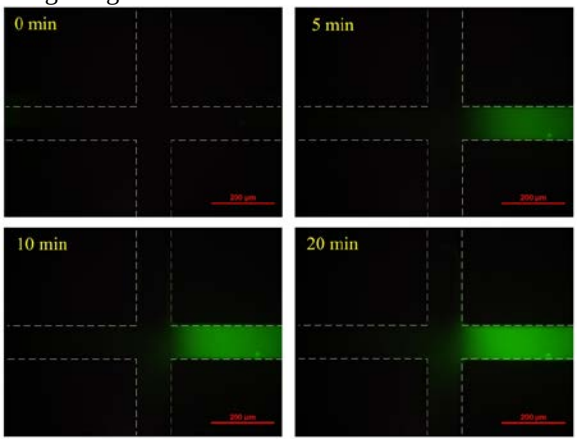

Fig. 5. Fluorescence images of 10 μM FITC-labeled BSA in 5 mM PBS solution taken at various time points.

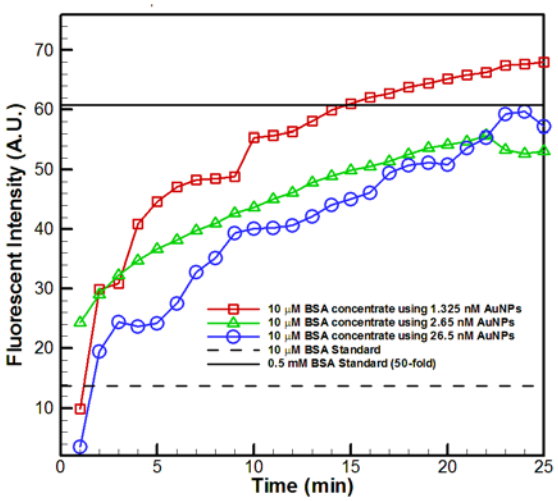

Fig. 6. Performance of protein preconcentration of 10 μM FITC-labeled BSA with different densities of gold nanoparticles.

The concentration performance for the initial protein concentration of 10 μM by the chip with different densities of gold nanoparticles is plotted in Fig. 6. Fluorescence intensity increases with time for all three samples due to the increased concentration of proteins. To estimate the final concentration, the fluorescence intensity of the standard BSA sample solutions (10 and 500 μM) was measured. Experimental results indicate that the protein sample with lower gold-nanoparticle concentration was concentrated more quickly than those with higher concentration. Fluorescent intensity also increases smoothly after a concentration time of 30 min for 10 μM FITC-labeled BSA using 1.325 nM gold nanoparticles. The equivalent value was then achieved at BSA standard concentration of 0.5 mM (approximately 50-fold the initial concentration). Therefore, a gold-nanoparticle concentration of 1.325 nM was the optimal condition for self-assembly. The capacity of proposed preconcentration microchip will

be improved by simple enhancement methods.

CONCLUSION

A rapid and simple microchip for protein preconcentration was fabricated by standard photolithography and PDMS microchannel production processes. The electrokinetic preconcentration of proteins was proven using nanofractures formed by gold nanoparticle-assisted electric breakdown at the junction gaps. Deposition of gold nanoparticles, which form SAM between the microchannels, was applied to reduce the electrical breakdown voltage. Nanofractures were created using driven DC voltages of as low as 50 V. In a current study, various gold-nanoparticle concentrations with the same mean diameter were used to collect 10 μM FITC-labeled BSA diluted in 5 mM PBS solution, with other conditions being similarly set in the experiments. The fluorescence intensity was recorded for 30 min to evaluate the performance of the chip. Results revealed that the protein samples were concentrated to approximately 50-fold of the initial concentration. The preconcentration speed was quicker, as the applied density of gold nanoparticles were lower. Moreover, a protein sample with a low initial concentration of 10 μM was concentrated to more than 50 times in just 15 min when gold nanoparticles were used at 1.325 nM concentration. The proposed chip may be used for rapid and low-cost protein preconcentration, and continuous development can enable the optimal parameters to be determined in succeeding steps.

ACKNOWLEDGEMENTS

The authors would like to thank the National Science Council of the Republic of China, Taiwan, for the financial support of this research under the following grants: MOST 105-2923-E-194-002-MY3 and MOST 105-2221-E-194-024-MY2.

REFERENCES

Chen, Y.H., Wu, H.F., Amstislavskaya, T.G., Li, C.Y., Jen, C.P., “A simple electrokinetic protein preconcentrator utilizing nano-interstices”; Biomicrofluidics, Vol. 10, pp. 24121(2016).

Duan, C., Wang, W., Xie, Q., “Review article: Fabrication of nanofluidic devices”; Biomicrofluidics., Vol. 7, pp. 26501(2013).

Islam, M.R., Serpe, M.J., “Label-free detection of low protein concentration in solution using a novel colorimetric assay”; Biosens. Bioelectron., Vol. 49, pp. 133–138(2013).

Jen, C.P., Amstislavskaya, T.G., Chen, K.F., Chen, Y.H., “Sample preconcentration utilizing nanofractures generated by junction gap breakdown assisted by self-assembled monolayer of gold nanoparticles”; PLoS ONE, Vol. 10, pp. 0126641(2015).

Jen, C.P., Amstislavskaya, T.G., Kuo, C.C., Chen, Y.H., “Protein preconcentration using nanofractures generated by nanoparticle-assisted electric breakdown at junction gaps”; PLoS ONE, Vol. 9, pp. 102050(2014).

Jeong, H.L., Chung, S., Sung, J.K., Han, J., “Poly(dimethylsiloxane)-based protein preconcentration using a nanogap generated by junction gap breakdown”; Anal. Chem., Vol. 79, pp. 6868–6873(2007).

Kim, S.M., Burns, M.A., Hasselbrink, E.F., “Electrokinetic protein preconcentration using a simple glass/ poly(dimethylsiloxane) microfluidic chip”; Anal. Chem., Vol.78, pp. 4779–4785(2006).

Koh, Y., Yang, J.K., Oh, M.H., Kang, H., Lee, Y.S., Kim, Y.K., “Nanoslit-concentration- chip integrated microbead-based protein assay system for sensitive and quantitative detection”; RSC Advanc., Vol. 7, pp. 29679–29685(2017).

Lee, J.H., Song, Y.A., Han, J., “Multiplexed proteomic sample preconcentration device using surface-patterned ion-selective membrane”; Lab Chip, Vol. 8, pp. 596(2008).

Lin, C.C., Hsu, J.L., Lee, G. B., “Sample preconcentration in microfluidic devices”; Microfluid. Nanofluid., Vol. 10, pp. 481–511(2011).

Pu, Q., Yun, J., Temkin, H., Liu, S., “Ion-enrichment and ion-depletion effect of nanochannel structures”; Nano Lett., Vol. 4, pp. 1099–1103(2004).

Quoc, T.V, Wu, M.S., Bui, T.T., Duc, T.C., Jen, C.P., “A compact microfluidic chip with integrated impedance biosensor for protein preconcentration and detection”; Biomicrofluidics, Vol. 11, pp.54113(2017).

Wang, C., Shi, Y., Wang, J., Pang, J., Xia, X.H., “Ultrasensitive protein concentration detection on a micro/nanofluidic enrichment chip using fluorescence quenching”; ACS App. Mat. Int., Vol. 7, pp. 6835–6841(2015).

Wang, J., Zhang, L., Xue, J., Hu, G., “Ion diffusion coefficient measurements in nanochannels at various concentrations”; Biomicrofluidics, Vol. 8, pp. 24118(2014).

Wang, Y.C., Stevens, A.L., Han, J., “Million-fold preconcentration of proteins and peptides by nanofluidic filter”; Anal. Chem., Vol. 77, pp. 4293–4299(2005).

Wu, D., Steckl, A.J., “High speed nanofluidic protein accumulator”; Lab Chip, Vol. 9, pp. 1890(2009).

Yang, R.J., Pu, H.H., Wang, H.L., “Ion concentration polarization on paper-based microfluidic devices and its application to preconcentrate dilute sample solutions”; Biomicrofluidics, Vol. 9, pp. 14122(2015).

Yu, H., Lu, Y., Zhou, Y., Wang, F., He, F., Xia, X., “A

simple, disposable microfluidic device for rapid protein concentration and purification via direct-printing"; Lab Chip, Vol. 8, pp.1496–1501(2008).

應用金奈米粒子自組裝薄膜於奈米流道電動力濃縮之金奈米粒子濃度測試

阮玉越 吳孟軒 任春平
中正大學機械工程學系

田能全
清華大學原子科學技術發展中心

摘要

本研究利用簡單且低成本方式，使用金奈米粒子自組裝方式沉積出奈米通道，用以達到蛋白質濃縮效果。晶片設計為十字型流道，並使用黃光微影製程製作母模，續以低成本且有良好生物相容性之聚二甲基矽氧烷(Polydimethylsiloxane, PDMS)轉印， 此晶片使用二次製程方法於特定位置自定義奈米通道位置，其區域使用APTES (3-aminopropyl-triethoxysilane)進行表面修飾，續將金奈米粒子自組裝(self-assembly)於晶片上，最後使用氧電漿接合技術使PDMS與玻璃基材相結合。實驗中採用不同濃度之15 nm金奈米粒子自組裝於晶片上，並使用10 μM 螢光異硫氰酸素(Fluorescein Isothiocyanate, FITC)標示之胎牛血清蛋白(Bovine Serum Albumin, BSA)進行濃縮，其結果顯示最佳合適濃度為稀釋0.5倍1.325 nM的金奈米粒子，且不同濃度之金奈米粒子須搭配不同濃度之緩衝液才能達到最好的濃縮結果。實驗發現搭配5 mM PBS所產生的電雙層效果最佳。進行電動力濃縮至30分鐘可將提升蛋白質濃度約50倍，順利將10 μM FITC-BSA提升至0.5 mM。